ICAS 2021 SHANGHAI
International Council of the Aeronautical Sciences
32nd Congress of the International Council of the Aeronautical Sciences
September 6-10, 2021
Pudong Shangri-La, Shanghai, China

The influence of the number of adhesive plies (FM 300-2) on fracture properties

J. Jokinen[1], M. Wallin[2], M. Kanerva[1]

[1]Tampere University, Faculty of Engineering and Natural Sciences, P.O.B 589, FI-33101 Tampere, Finland
[2]Patria Aviation, Lentokonetehtaantie 3, FI-35600 Halli, Finland

Abstract

Adhesively bonded joints, their strength and fracture properties, are influenced by several factors of design and material. One main factor is the thickness of the bond line, i.e. thickness of the adhesive layer. In this work, three methods of experimental testing are used for studying the influence of adhesive thickness. These tests are the butt joint method, double cantilever beam method, and end notched flexure method. These test methods target to determine the out-of-plane strength and fracture energies for the fracture modes I and II. This work presents these experiments and the test results with one FM 300-2 (Solvay) ply of adhesive applied to the test specimens. Specimens with two plies of the FM 300-2 adhesive have been tested and the results published in the current literature. Finally, the comparison between the results related to the specimens with one and two adhesive plies are compared based on this study and literature.

Keywords: adhesive thickness; strength; fracture test; FM 300-2; virtual crack closure technique

1. Introduction

Strength and fracture energy (term fracture toughness is also typical, e.g. by ASTM standards) are important material properties when describing the mechanical behaviour of adhesive, bonded joints. Strength and fracture energy in the bonded joint are in details influenced by many factors, such as the surface treatment applied to adherends [1] and the chemo-physical configuration of the adhesive product used [2]. Typically, the thickness of the adhesive layer between adherends is required to be adequate – naturally the minimum is that the adherend surfaces are evenly wetted. The thickness of the adhesive layer has shown to have significant influence on the strength of bonded joint [3] and fracture process [4]. Lee et al. [5] have classified adhesives into two typical types in terms of the thickness versus fracture energy behaviour. For the first type, the fracture energy is monotonically growing when the thickness is increased. For the second type, the fracture energy tends to decrease after certain value of thickness is achieved.

Structural bonding in aeronautical applications is typically performed using film adhesives. Adhesive plies are not always consisting of pure adhesive but can also include carrier cloths to control the thickness of the adhesive in a joint. Carrier cloths also improve the handling of the adhesive in practice. Carrier cloths have been studied in the current literature. Forte et al. [6] stated that a typically carrier (cloth) is not intended to enhance mechanical properties. Sargent [7] studied the modifications of neat resin using PEEK monofilaments and aramid fibres – the comparison of fracture energy values (double cantilever beam method, DCB) showed remarkably higher values for the modified specimens.

A wide range of testing methods for the adhesively bonded joints' (in terms of strength) have been developed over the years by the field of adhesion and adhesives. Traditional specimens are the single and double lap joints tested under tensile loading. The stress distribution in these specimens is a combination of peel and shear stresses. The adhesives' out-of-plane strength is typically measured using the butt joint (BJ) specimen. In practice, the BJ specimen has a three-dimensional stress state that is more pronounced at the edges of the bond (cross-section) [8]. During recent

years, the focus of adhesive damage has been important in the development of the fracture testing. The mode I fracture energy (G_{Ic}) have been long determined by using the DCB-based methods [9]. The mode II testing has still more variation in the systematic procedures but the end notched flexure (ENF) testing has become popular [10].

This work focuses on the out-of-plane strength and the fracture energy of fracture modes I and II. The target of the work is to study the influence of the adhesive layer's thickness on the properties. The applied adhesive product is an epoxy-based adhesive ply FM 300-2 (Solvay). This adhesive ply includes knitted carrier. This work presents experimental results for bonded specimens with one adhesive ply (BJ, DCB, and ENF methods). The same experimental methods have been applied to specimens with two adhesive plies per bond in the current literature. In this work, the quantitative measures are analysed by the comparison between one and two adhesive plies.

2. Materials and methods

2.1 Materials

The adhesive used was an epoxy-based film adhesive FM 300-2 (Solvay). Adhesive's material properties were estimated for numerical analysis based on the product FM 300-K [11]; Young's modulus was anticipated 2.45 GPa and Poisson's ratio 0.38. The adherend was an aluminium alloy in all specimens. The alloys were Al6082-T6, Al7075-T76, and Alumec 89 (Uddeholm) applied to BJ, DCB, and ENF specimens, respectively. Aluminium alloys' properties were estimated by using Young's modulus of 71 GPa and Poisson's ratio of 0.33 [12].

2.2 Butt joint (BJ) tests

Six BJ specimens were tested using the cylindrical specimen geometry as shown in Figure 1. The average measured diameter was 14.74 mm providing the average cross-sectional area of 170.64 mm^2. BJ specimens had one adhesive ply, which had an average thickness of 0.25 mm. The aluminium adherends were coated by the DIARC Bindo coating [1] prior to bonding to ensure firm adhesion. The testing was performed with a 100 kN (load cell) tensile testing machine (MTS). The displacement rate was constant (2 mm/min), as described in a study [13].

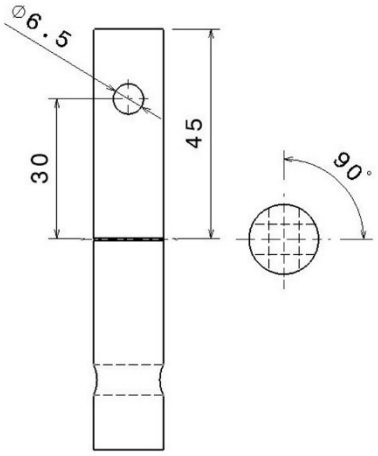

Figure 1. The dimensions of the BJ test specimen [13].

The average out-of-plane strength was calculated by using the equation

$$\sigma = \frac{F}{A} \tag{1}$$

where F is the maximum ('peak') force and A is the cross-sectional area of the BJ specimen.

2.3 Double cantilever beam (DCB) tests

The DCB specimen of this study consisted of one adhesive ply used for bonding, two adherends and loading blocks. The initial crack was created using an insert film. The insert film was positioned above the adhesive ply. This process selection caused a slight asymmetry for the DCB specimens in terms of initial crack tip's location. The loading blocks were attached at the specimen end where the initial crack exists. The DCB specimens' dimensions are presented in Figure 2. The average measured initial crack length (from the specimen end to the tip of crack) and specimen width were 65.47 mm and 19.99 mm, respectively. Six DCB specimens were tested. The same tensile testing machine than in case of the BJ testing was used. The force (U2B/500N, HBM) and displacement (WA-L 50 mm, HBM) transducers were used in the testing to collect data.

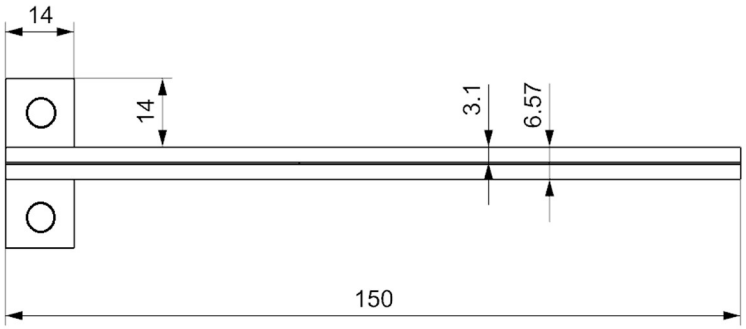

Figure 2. The DCB test specimen's dimensions in this study.

The DCB tests are analysed to calculate the fracture energy, G_{IC}, by using the corrected beam theory (CBT) [9]. The CBT equation can be extracted as

$$G_{\mathrm{I}} = \frac{3P\delta}{2B(a+|\Delta|)} \cdot \frac{F}{N} \tag{2}$$

where P is the force (opening), δ is the displacement (opening at loading blocks), B is the width, a is the crack length, and F, N and Δ are fitting parameters.

The DCB testing is performed in two load cycles as defined in the standard procedure. The crack is propagated a few millimetres from the pre-existing crack tip in the first cycle. The initiation-related G_{IC} value is defined by this cycle. The crack is forced to propagate 60 mm further in the second load cycle. The fracture energy is evaluated with different (momentary) crack lengths. Typically, the second cycle's fracture energy is called as the propagation value and presented using an average G_{IC} value. However, the fracture energy can be dependent on the crack length, which has led to the development of sophisticated descriptions. Ameli et al. [14] presented the bi-linear model for the fracture energy evaluation. In the first part of this model, the fracture energy increases until a stable value. After reaching the stable value, the curve is modelled as a plateau. In a mathematical form, the bi-linear model can be extracted

$$G_{\mathrm{C}} = \begin{cases} G_{\mathrm{ci}} + dG_{\mathrm{cr}}/da(a-a_0), & a_0 < a < a_{\mathrm{r}} \\ G_{\mathrm{cs}}, & a \geq a_{\mathrm{r}} \end{cases} \tag{3}$$

where G_{cs} is the stable value, G_{ci} is the initiation value, a_0 is the initial crack length, and a_{r} is the crack length where the plateau part begins.

2.4 End notched flexure (ENF) tests and FE modelling

The mode II related fracture energy (G_{IIC}) can be determined with the ENF testing method. The ENF specimen was tested by using the three-point bending fixture and by using the 100 kN tensile testing machine (MTS) mentioned above. Auxiliary force transducers (20 kN range) were applied to both lower supports of the fixture. The displacement transducer was positioned under the mid-point of the specimen (span). The specimen's dimensions are shown in Figure 3. One adhesive ply was used for bonding and the adhesive thickness (measured) was 0.35 mm, the pre-crack length was 108.61 mm, and the specimen's width (measured) 17.00 mm. Six specimens were tested.

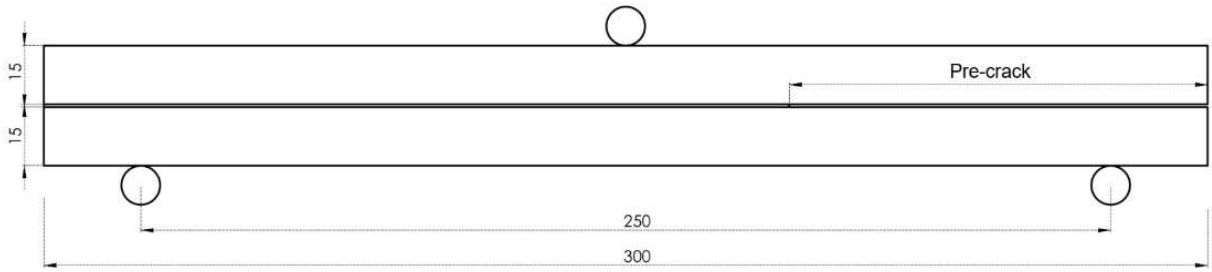

Figure 3. The dimensions of the ENF test specimen [15] as used in this study.

A large number of analytical methods for evaluating the fracture energy (G_{IIC}) are presented in the current literature. In our approach, the evaluation was performed using the Virtual Crack Closure Technique (VCCT) as a method in FE simulation. The average ENF specimen of our experimental series was modelled using Abaqus/Standard 2017. The applied FE model is shown in Figure 4. The ENF model consisted of adherends and adhesive. The tie constraint was executed for the lower interface between the adhesive part and an adherend. The VCCT was executed for the upper interface between the adhesive part and an adherend. The boundary conditions were placed at the support locations matching the loading noses of the fixture in real tests. The vertical and width directions' displacements were restricted in both locations while the longitudinal displacement was restricted only for the intact end (support loading nose) of the specimen. The loading was created into the middle of the specimen, in details the nodal points. The sum of nodal point-concentrated force values was equal to the experimental peak load (average of series). The typical element in the adhesive was 2.5 mm (C3D8R) and adherends 0.35 mm (C3D8I).

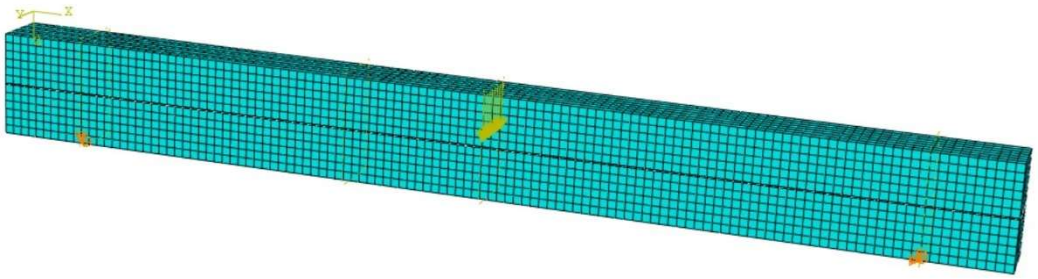

Figure 4. The finite element model of the ENF specimen.

2.5 Two adhesive plies – reference experiments of literature

This paper presents results related to specimens with only one adhesive ply. Similar specimens with two adhesive plies for BJ, DCB, and ENF testing have been studied and the results published in studies rather recently [13], [15] & [16]. The test arrangements in the mentioned literature were essentially identical except for the number of adhesive plies. All the tests for different types of methods included six specimens. It should be noted that the insert film could be placed symmetrically between (two) adhesive plies in the DCB and ENF specimens with two adhesive plies. The arrangement with only one ply theoretically provides slight asymmetry in terms of the location of pre-crack and adhesive that bonds to one of the adherends under the piece of insert film.

3. Results

3.1 Analysis of BJ tests

The fracture surfaces of BJ specimens are shown in Figure 5. The fracture surfaces represent mainly cohesive failure. The average maximum force of the BJ testing was 5.88 kN ± 0.75 kN. This corresponds the average out-of-plane strength of 34.49 MPa ± 4.36 MPa.

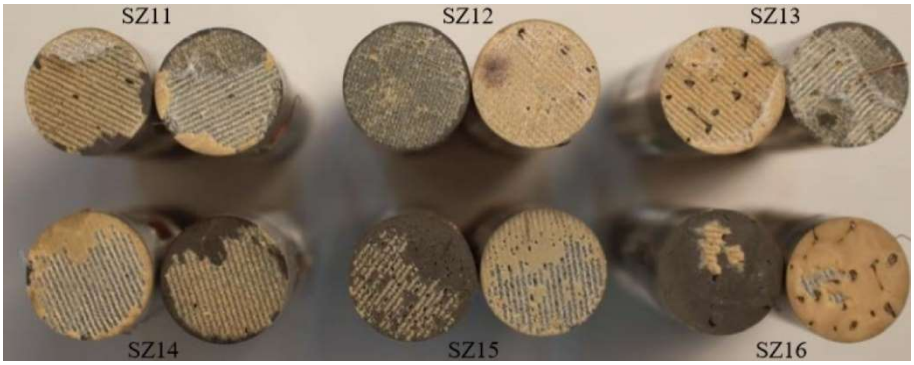

Figure 5. The fracture surfaces of BJ test specimens in this study.

3.2 Analysis of DCB tests

The evaluated DCB force-displacement curves are shown in Figure 6 and 7. The curves of all the specimens are closely consistent. Figure 6 describes the first load cycle where the crack propagation is small. This is remarked by a small nonlinear part in the curve before the unloading starts. Figure 7 presents the second load cycle where the crack propagates from the natural crack front (created during the first cycle). The initial part in these curves is linear before the crack propagation. The nonlinear part of these curves differs when compared to the typical DCB specimens' curves. In the 'typical' DCB curve, the force starts decreasing in a parabolic manner after reaching the maximum force. The increase or a plateau is clear in our experiments after reaching the nonlinear point (instead of the decreasing force). The decrease of force started only when reaching approximately 15 mm of displacement.

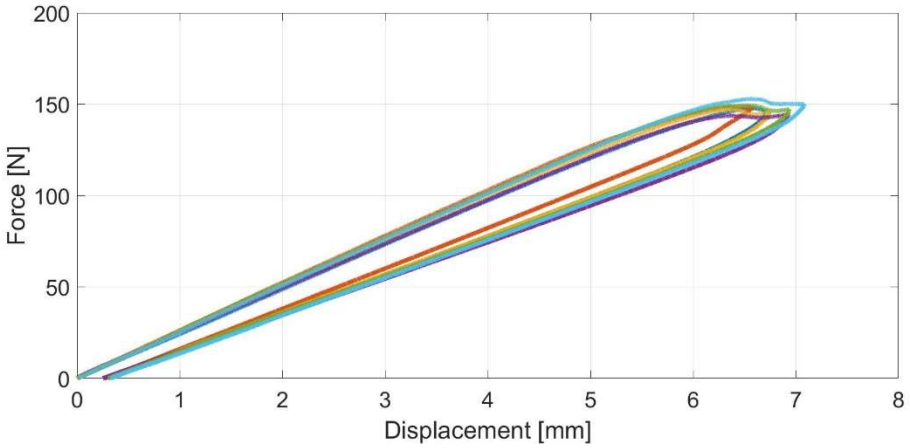

Figure 6. The DCB tests: the first load cycle and the force-displacement curves.

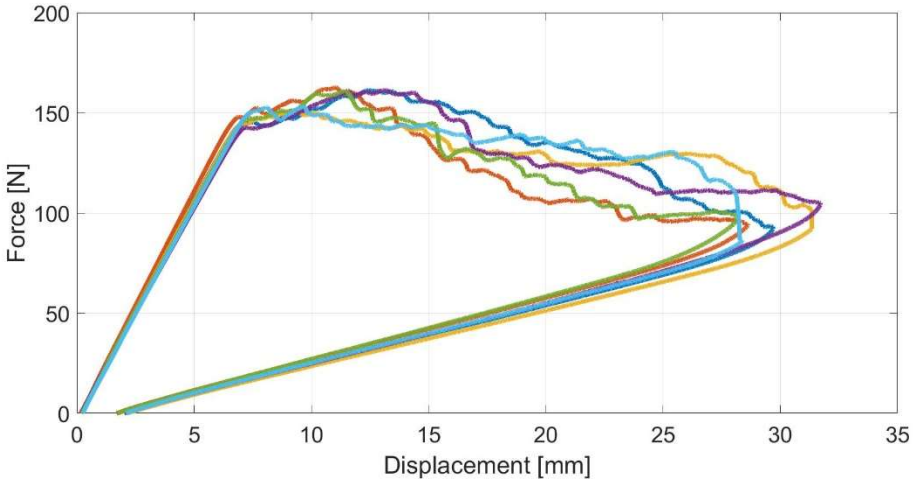

Figure 7. The DCB tests: the second load cycle and the force-displacement curves.

G_{IC} values were computed using the CBT equation (Eq. 2). The DCB test is initiated from the pre-existing artefact crack during the first cycle. The initiation G_{IC} value was calculated at the point when the crack starts to propagate during the first load cycle. The initiation was defined based on the visual observation of crack on the side of the specimen. The initiation value was 1038.7 J/m^2 in average here. The DCB testing in the event of the second load cycle provides the propagation value. The experimental fracture energies calculated for different momentary crack lengths are shown in Figure 8. The experimental fracture curve and its values at the plateau part range from 1400 J/m^2 to over 2300 J/m^2. The total average fracture energy for the second cycle was 1723.2 J/m^2. Also, the bi-linear model [14] was fitted for the propagation values. The bi-linear model's increasing phase-related crack length is 16.3 mm (=a_r). During this phase, the ERR increased from 1001.3 J/m^2 (G_{ci}) to 1819.7 J/m^2 (G_{cs}) here. The fitted bi-linear model is also shown in Figure 8.

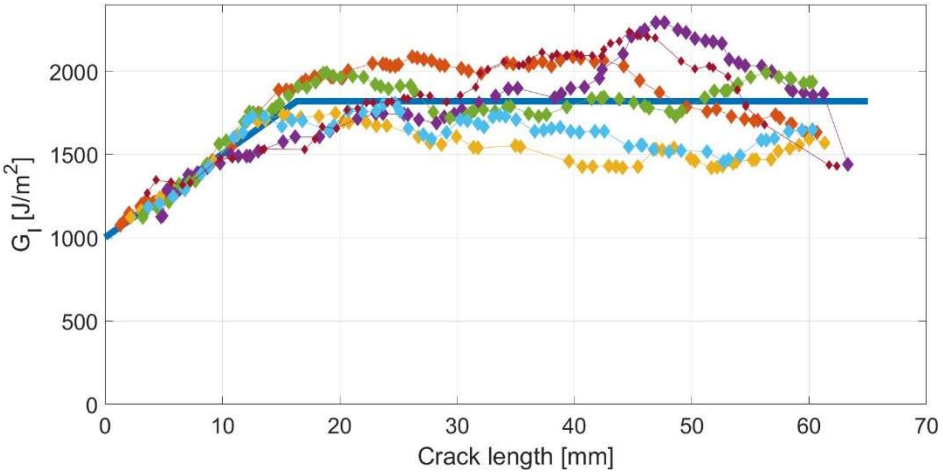

Figure 8. The DCB tests: the second load cycle and its fracture energy calculated for momentary crack lengths – experiments and the bi-linear model shown (blue line).

3.3 Analysis of ENF tests

The ENF tests and the force-displacement curves are shown in Figure 9. The similarity between the test specimens in terms of their force-displacement data can be clearly seen. The experimental curves provide a nonlinear rising part which reaches the maximum force before any force drop is shown. Furthermore, the force grows after a drop is reached and when the enforced displacement continues (the constant test rate). The average maximum force value before the drop 'hump' is 8525 N and the standard deviation is 90 N.

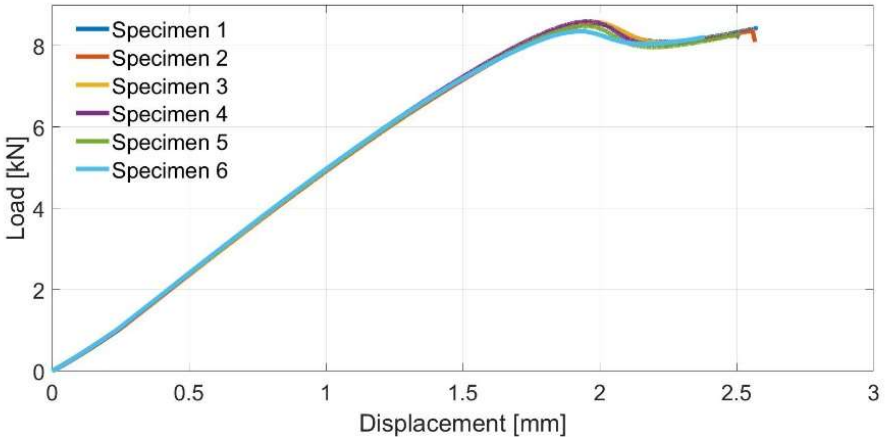

Figure 9. The experimental ENF testing in the form of force-displacement curves.

The ENF testing provides in general only one G_{IIC} value because the crack propagation is not observed after the onset. The G_{IIC} value was here determined using the VCCT analysis and with the average experimental force value (8525 N). Figure 10 presents the G_{IIC} distribution provided by the three-dimensional VCCT analysis. The G_{IIC} distribution shows high peaks at the specimen edges, which are limited to an element length in our work (our FE model). The representative G_{IIC} was taken as the value by the middle nodal point. This selection follows the approach applied in the work by Jokinen et al. [15]. Here, the middle point's G_{IIC} value was 4897 J/m^2.

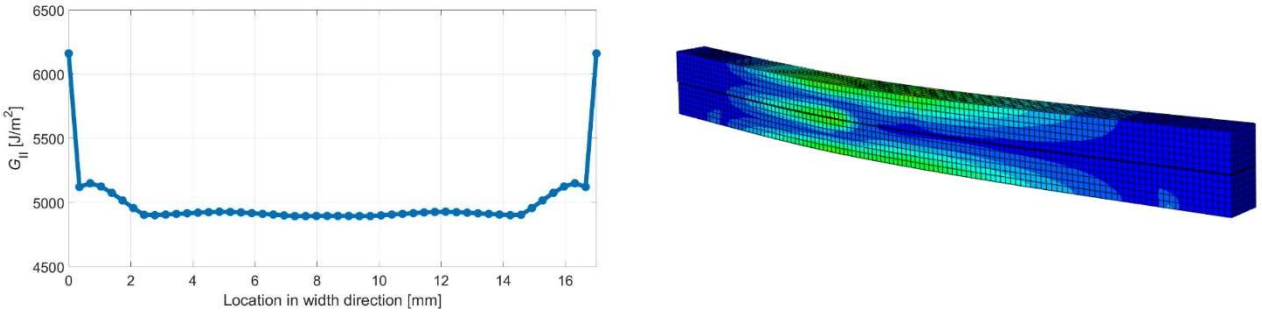

Figure 10. The G_{II} distribution provided by the FE simulation and the VCCT analysis (left). The ENF analysis von Mises distribution (right).

3.4 Comparison of current work and literature data

The comparison of tests for specimens with one and two adhesive plies per specimen are shown in Table 1. The comparison reveals that the usage of two plies leads to a decrease in the out-of-plane strength (26% increase when only one ply). This is an opposite trend than what is observed in the results of DCB and ENF tests. The one ply-related DCB specimen resulted in lower initiation value than the specimens with two plies (DCB). The bi-linear fracture energy curve in one ply-related tests was another difference found for the DCB testing: The bi-linear model / fitting is meaningless in the case of two plies per specimen. However, the propagation values (DCB) are similar for specimens with either one or two plies. Actually, the plateau for the bi-linear model (one ply) is considered in these values. The ENF method-related comparison indicates clearly higher values for the specimens with two adhesive plies than those with one adhesive ply (21% decrease when only one ply).

Table 1. The comparison between the experiments of this study (one adhesive ply per specimen) and the literature (two adhesive plies per specimen).

	One ply applied	Two plies applied [13], [15] & [16]	Difference compared to two plies applied [%]
BJ: σ_{IC}	34.49 MPa	27.35 MPa	26.1
DCB: initiation G_{IC}	1038.7 J/m^2	1604 J/m^2	-35.3
DCB: propagation G_{IC}	1819.7 J/m^2	1820 J/m^2	-0.1
ENF: G_{IIC}	4897 J/m^2	6230 J/m^2	-21.4

4. Discussion

Structural adhesive bonding is typically performed by using film adhesive so that the number of plies stacked is relevant. The adhesive's thickness can be controlled by the number of plies when the film product contains a carrier system (such as cloth or fabric). Of course, the manufacturing pressure can also influence on the adhesive thickness. Different areal masses and thicknesses might also exist for commercial products. Typically, the bonding is made using one adhesive ply due to the easiness and faster process time. However, some repairs and its instructions require two plies for providing feasible bond line. The usage of two or more plies is not a common approach but could affect mechanical durability. Based on the results of this work, the fracture behaviour can be improved when using two adhesive plies. The increase in the initiation values of fracture energy (fracture toughness) is over 20 percent for the specimens of this study. This is a clear improvement but the increased number of plies has drawbacks. The usage of more plies increases the complexity of manufacturing and also mass of the bonded joint. The starting point of crack for both DCB and ENF tests is the initial pre-existing crack. The likelihood of pre-existing cracks in real structures, or other defects, in adhesive joints should be studied and compared for joints with either one or two adhesive plies in future. This type of future study could clarify the importance of the gained fracture energy development and provide further manufacturing or repair recommendations for the number of adhesive plies.

5. Conclusion

In this work, the influence of the number of adhesive plies applied to adhesive joints and in term of the out-of-plane strength and fracture energy for the fracture modes I and II were analysed. The results show that the number of plies has an influence on the out-of-plane strength and the fracture energy for modes I and II. In the BJ testing, two adhesive plies per specimen resulted in lower out-of-plane strength than when one ply had been used. The fracture mode I related testing indicated a lower initiation fracture energy when having only one ply instead of two. The fracture energy data in this work, with one ply, had a bi-linear relation. After the rising part of the curve (mode I), the DCB specimens with one ply provided very similar fracture energy than the specimens with two plies. Two plies per specimen tended to provide a higher fracture energy than the use of one ply per specimen for the mode II ENF testing.

6. Acknowledgements

Authors want to acknowledge Finnish Defence Forces Logistics Command for the financial support.

7. Contact Author Email Address

mailto: jarno.jokinen@tuni.fi

8. Copyright Statement

References

[1] Aakkula J, Jokinen J, Saarela O and Tervakangas S, Testing and modelling of DIARC plasma coated elastic-plastic steel wedge specimens, *International Journal of Adhesion and Adhesives*, Vol. 68, pp. 219-228, 2016.

[2] Burkholder G, Kwon Y and and Pollak R, Effect of carbon nanotube reinforcement on fracture strength of composite adhesive joints, *Journal of Materials Science*, Vol. 46, pp. 3370–3377, 2011.

[3] Naito K, Onta M and Kogo Y, The effect of adhesive thickness on tensile and shear strength of polyimide adhesive, *International Journal of Adhesion and Adhesives*, Vol. 36, pp. 77–85, 2012.

[4] Banea M, da Silva L and Campilho R, The Effect of Adhesive Thickness on the Mechanical Behavior of a Structural Polyurethane Adhesive, *The Journal of Adhesion*, Vol. 91, pp. 331-346, 2015.

[5] Lee D-B, Ikeda T, Miyazaki N and Choi N-S, Effect of bond thickness on the fracture toughness of adhesive joints, *Transactions of the ASME*, Vol. 126, pp. 14–18, 2004.

[6] Forte MS, Whitney JM and Schoeppner GA, The influence of adhesive reinforcement on the Mode-I fracture toughness of a bonded joint, *Composites Science and Technology*, Vol. 60, pp. 2389–2405, 2000.

[7] Sargent J, The influence of inclusions on the strength of the adhesive, *International Journal of Adhesion and Adhesives*, Vol. 26, pp. 151–161, 2006.

[8] Jokinen J and Kanerva M, Cohesive zone modelling of adhesive in butt joint specimen, *5th International Conference on Integrity – Reliability – Failure*, Porto/Portugal, 24-28 July, 2016

[9] ISO 25217, Adhesives – Determination of the mode 1 adhesive fracture energy of structural adhesive joints using double cantilever beam and tapered double cantilever beam specimens, *International Organization for Standardization*, 2009.

[10] Blackman B, Kinloch A and Paraschi M, The determination of the mode II adhesive fracture resistance, G_{IIC}, of structural adhesive joints: an effective crack length approach, *Engineering Fracture Mechanics*, Vol. 72, pp. 877–897, 2005.

[11] Ishai O, Rosenthal H, Sela N and Drukker E, Effect of selective adhesive interleaving on interlaminar fracture toughness of graphite/epoxy composite laminates, *Composites*, Vol. 19, pp. 49–54, 1988.

[12] MIL-HDBK-5J, Metallic materials and elements for aerospace vehicle structures, *Military Handbook*, Department of Defence, USA, 2003.

[13] Jokinen J, Kanerva M, Wallin M and Saarela O, The simulation of a double cantilever beam test using the virtual crack closure technique with the cohesive zone modelling, *International Journal of Adhesion and Adhesives*, Vol. 88, pp. 50–58, 2019.

[14] Ameli A, Papini M, Schroeder JA and Spelt JK, Fracture R-curve characterization of toughened epoxy adhesives, *Engineering Fracture Mechanics*, Vol. 77, pp. 521–534, 2010.

[15] Jokinen J, Orell O, Wallin M and Kanerva M, A concept for defining the mixed-mode behaviour of tough epoxy film adhesives by single specimen design, *Journal of Adhesion Science and Technology*, Vol. 34, pp. 1982-1999, 2020.

[16] Jokinen J, Wallin M and Saarela O, Applicability of VCCT in mode I loading of yielding adhesively bonded joints – a case study, *International Journal of Adhesion and Adhesives*, Vol. 62, pp. 85-91, 2015.